Edges of flames that don't exist

R. W. Thatcher and J. W. Dold

Mathematics Department, UMIST, Manchester M60 1QD, Britain
<R.W.Thatcher@UMIST.ac.uk>

Abstract

A counterflow diffusion flame model is studied revealing that, at least as a part of the quenching boundary is approached in parameter space at low enough Lewis numbers, an edge of a diffusion flame, or triple flame, has a propagation speed that still advances the burning solution into regions that are not burning. In crossing the quenching boundary, the advancing flame edge remains a robust part of the solution but the flame behind the edge is found to break up into periodic regions, resembling "tubes" of burning and non-burning, accompanied by the appearance of an oscillatory component in the speed of propagation of the edge. In crossing a second boundary the propagation speed of the flame edge disappears altogether. The only unbounded, non-periodic stationary solution then consists of an isolated flame tube although stationary periodic flame tubes can also exist under the same conditions. In passing back through parameter space, starting with a single flame tube already present, there is no sign of hysteresis and the oscillatory edge propagation reappears at the same point where it disappears. On the other hand, in continuing forwards across a third, final boundary the flame tube is extinguished leaving no combustion whatever. Boundaries in parameter space where different solutions arise are mapped out.

1 Introduction

A flame can possess an edge whenever a reactive setup is able to sustain both burning and non-burning as steady solutions [1]–[4]. Normally, these two solutions each vary in only one direction, a spatial coordinate normal to the flame, and are uniform in all other directions. By considering a two or three dimensional region where burning meets non-burning, a structure arises in which the flame comes to an end and gives way to the non-burning state.

Triple flames are examples of this kind of structure (see [4] and references therein), arising where a diffusion flame comes to an end, but flame edges could also arise in many other circumstances including either fresh-to-fresh or fresh-to-burnt strained premixed flames with nonadiabatic losses, partially premixed flames and cylindrical or tubular flames [5]. All that is needed is the existence of multiple steady-state solutions that are uniform in all but one spatial variable. Different pairs of such solutions provide far-field boundary conditions which determine the states to be found on either side of the flame edge.

A pertinent feature of the flame edge is that it has the ability to propagate, even where the flame, of which it is an edge, is intrinsically unable to do so, such as a diffusion flame. Under the influence of various control parameters in the system, such as strain rate, Damköhler number, Lewis Numbers, heat loss parameters, etc., the edge can propagate either positively, extending the flame, or negatively, representing the encroachment of a quenched state into regions that are otherwise burning. A general discussion, including some dynamical and statistical aspects in randomly varying fields, can be found in [4].

In two dimensions (x, y) a typical model for flame edges in a velocity field (v, w), where we will take v to be single signed, can be written in the dimensionless form

$$f_t + vf_x = (df_x)_x + \mathcal{R}(f) \qquad \text{with} \qquad \mathcal{R}(f) = \delta R(f) + (df_y)_y - wf_y. \tag{1}$$

where $f(t,x,y)$ is a vector of fluid and chemical properties, $R(f)$ represents a vector of chemically reactive source terms, with Damköhler number δ, and d is a diffusivity matrix. When set to zero the operator $\mathcal{R}(f)$ is the restriction of the problem to uniformity in x and in time t, so that $\partial_t = \partial_x = 0$. Note that the model (1) assumes uniformity in the third z-direction in which an outgoing straining flow may occur, with w typically representing an inflow. Given suitable boundary conditions such as, $f(t,x,\pm\infty) = f^{\pm}$, "front" and "back" equilibrium states $f_{\rm f}(y)$ and $f_{\rm b}(y)$ that are uniform in x and t satisfy $\mathcal{R}(f_{\rm f}) = \mathcal{R}(f_{\rm b}) = 0$. If we take $f_{\rm b}$ to represent a "burning" state with a reaction rate vector $R(f)$ that is typical of combustion problems, then the solution $f_{\rm b}$ generally only exists above a quenching Damköhler number $\delta_{\rm q}$ and, depending on the nature of $R(f)$, the solution $f_{\rm f}$ might only exist below an ignition Damköhler number $\delta_{\rm i}$.

Within the range $\delta_{\rm q} < \delta < \delta_{\rm i}$, a flame edge problem that represents a transition between $f_{\rm f}$ and $f_{\rm b}$ is then easily formulated by choosing these states as far field boundary conditions in x, in the manner $f(t,-\infty,y) = f_{\rm f}(y)$ and $f(t,\infty,y) = f_{\rm b}(y)$; the appropriate far field conditions in y remain $f(t,x,\pm\infty) = f^{\pm}$. In any steady solution (having $\partial_t = 0$), the propagation speed of the flame edge in the x-direction may be defined as the value of v at some suitably representative point, such as $v(\,\cdot\,,-\infty,0)$, and this speed is generally an eigenvalue of the nonlinear problem, allowing solutions to exist only for one particular value, unless either $f_{\rm f}$ or $f_{\rm b}$ is unstable in which case there should be an unbounded continuous spectrum of eigenvalues in a half space [2, 4]. Integrating at any fixed value of y for any component of f gives

$$\int_{f_{\rm f}}^{f_{\rm b}} v\,df = \int_{-\infty}^{\infty} \mathcal{R}(f)\,dx \qquad \text{or} \qquad \int_{-\infty}^{\infty} v f_x^2\,dx = \int_{f_{\rm f}}^{f_{\rm b}} \mathcal{R}(f)\,df. \tag{2}$$

The values of $\mathcal{R}(f)$ can change sign in many ways between the equilibrium states $f_{\rm f}$ and $f_{\rm b}$ so that even if the appropriate component of the reaction rate function $R(f)$ is single signed these relationships do not determine the sign of v as they would in similar relationships applied to one dimensional propagating flames, for which $\mathcal{R}(f) \equiv R(f)$.

For continuity reasons [2]–[4], one might expect v to be negative (representing non-burning encroaching into the burning solution) near $\delta = \delta_{\rm q}$. This is found to be the case in studies of triple flames for Lewis numbers of unity [1, 6]. However, it is not always the case as will be demonstrated for the non-premixed combustion model studied in this article.

In some parameter ranges we find that v can remain positive as δ decreases towards $\delta_{\rm q}$. Indeed, although the notion of a flame edge as a boundary between burning and non-burning loses its meaning when $\delta < \delta_{\rm q}$ (since the solution $f_{\rm b}$ ceases to exist) we show that a flame edge solution of a kind does continue to exist as long as v is positive at the point where the flame behind it ceases to exist. In effect, a flame edge that is propagating so as to spread burning does not immediately give up its job as soon as the flame that it produces runs into difficulty. Instead, we find that the positive propagation speed becomes oscillatory in time and the flame that remains behind the edge breaks up into a series of separated, non-propagating regions of burning.

In moving further from the boundary $\delta = \delta_{\rm q}$ a stage is reached where we find that flame edges no longer propagate and, instead, one or more isolated and stationary regions of burning can persist, each sustained by two non-propagating flame edges. For non-premixed burning these pairs of flame edges take the form of linked triple flames, so that some, albeit weak connection exists between the premixed flame branches of each one. Remembering that the solutions are uniform in the third z-dimension, the flames resemble tubes of burning having an oval cross-section with a diffusion flame linking opposite sides of the oval. This form of solution is ultimately lost in moving yet further from the boundary into a regime where no form of combustion at all seems to be possible. The boundaries in parameter space between these different modes of combustion are mapped out numerically. Results of this nature were first presented in [7].

Some analogous observations were made more recently in premixed models for flame edges [8, 9] and isolated regions of burning have been observed experimentally [10] for both premixed and non-premixed cases at low Lewis numbers and suitable Damköhler numbers or strain rates. Interestingly, Daou and Liñán [8] observed that isolated burning regions, which they refer to as spots of combustion, can be found even for some Lewis and Damköhler numbers where the one dimensional flame solution, for which $\mathcal{R}(f_{\rm b}) = 0$, does still exist and any edge of such a flame has a negative propagation speed; a similar observation arises with non-premixed combustion although details are not presented in this article. Also using a premixed model, Buckmaster and Short [9] argue that the appearance of separated regions of burning, which they call flame strings, is associated with an instability of the uniform one dimensional flame, arising from a periodic spatial disturbance along the flame surface that first appears close to quenching at low enough Lewis numbers.

Thatcher et al [7] described the separated regions of burning that they observed for non-premixed combustion as segments. Ronney and co-workers [10] use the term flame tubes to refer to isolated regions of burning in both premixed and non-premixed situations. Cylindrical flames, also called tubular flames, as examined in [5], are confined by a cylindrically symmetric incoming flowfield while the flame tubes observed by Ronney are confined by a competition between quenching and a positive edge propagation speed that is enhanced by a higher diffusivity of reactants than heat, as described here. Both mechanisms lead to similar results so that it seems suitable to retain the descriptive term "flame tube" to unify the various terminologies that different authors have adopted independently.

A fully developed bifurcation starting from the appearance of a linear instability in the one dimensional flame, as suggested by Buckmaster and Short [9], could certainly persist beyond the point of quenching. Such an instability, close to quenching at low enough Lewis numbers, is already known to exist for non-premixed combustion [11] and is likely to be related to the appearance of the flame tubes that we have also observed [7]. However, a more detailed study of the bifurcations involved would be needed to establish the connection more directly. In this article, we observe that flame tubes appear as the result of an unsteady dynamic evolution in the propagation of a flame edge when entering a region of parameter space where the one dimensional flame ceases to exist while the propagation speed of the flame edge remains positive. Strictly speaking, this is a different mechanism and it is not clear, for example, that the same wavelength would be selected as that associated with the strongest mode of linear instability of the one dimensional flame at or near the point of quenching. Moreover, we also identify isolated flame tubes, as did Daou and Liñán [8] for a premixed model, that could not arise directly from a periodic instability. We go on to provide some mapping of the parameter space within which different types of solution appear.

2 A diffusion flame edge model

We consider numerical solutions of the following diffusion flame edge or triple flame model for general Lewis numbers $L_{\rm F}$ and $L_{\rm X}$ of fuel and oxidant respectively

$$\begin{aligned} \frac{\partial}{\partial t}\begin{pmatrix} Y_{\rm F} \\ Y_{\rm X} \\ T \end{pmatrix} + S\frac{\partial}{\partial x}\begin{pmatrix} Y_{\rm F} \\ Y_{\rm X} \\ T \end{pmatrix} &= \frac{\partial^2}{\partial x^2}\begin{pmatrix} Y_{\rm F}/L_{\rm F} \\ Y_{\rm X}/L_{\rm X} \\ T \end{pmatrix} + \mathcal{R} \\ \mathcal{R} &= y\frac{\partial}{\partial y}\begin{pmatrix} Y_{\rm F} \\ Y_{\rm X} \\ T \end{pmatrix} + \frac{\partial^2}{\partial y^2}\begin{pmatrix} Y_{\rm F}/L_{\rm F} \\ Y_{\rm X}/L_{\rm X} \\ T \end{pmatrix} + \delta\begin{pmatrix} -1 \\ -1 \\ 2 \end{pmatrix}\beta^3\, Y_{\rm F} Y_{\rm X}\, T^{\beta} \end{aligned} \tag{3}$$

in which $Y_{\rm F}$, $Y_{\rm X}$ and T represent scaled fuel and oxidant concentrations and temperature. Dimensionless lengths and time are chosen such that the single converging component of the strain rate, namely the rate at which the y-component of velocity varies with y, is exactly -1. The Damköhler number δ is then inversely proportional to the actual dimensional value of the strain rate. There is no component of strain in the x-direction and a strain component of $+1$ must exist in the z-direction for the flow to be incompressible. For simplicity it is assumed that the density remains constant, an assumption that is known to reproduce many important aspects of the physics qualitatively well in reactive-diffusive systems [12]. It is also assumed that there is no shear, that the strain rate field is uniform and that $Y_{\rm F}$, $Y_{\rm X}$ and T are all uniform in the z-direction so that it is only necessary to consider two spatial directions and time in the model.

Far field boundary conditions representing an inflow of cold fuel from $y = \infty$ and cold oxidant from $y = -\infty$ can be written as

$$\lim_{y\to\infty}\begin{pmatrix} Y_{\rm F} \\ Y_{\rm X} \\ T \end{pmatrix} = \begin{pmatrix} Y_{\rm F0} \\ 0 \\ 0 \end{pmatrix}, \qquad \lim_{y\to-\infty}\begin{pmatrix} Y_{\rm F} \\ Y_{\rm X} \\ T \end{pmatrix} = \begin{pmatrix} 0 \\ Y_{\rm X0} \\ 0 \end{pmatrix}. \tag{4}$$

There is a symmetry about $y = 0$ if $Y_{\rm F0} = Y_{\rm X0} = 1$, and $L_{\rm F} = L_{\rm X} = L$, and for simplicity this is the choice of parameters used in the numerical investigations made so far. In the results presented in this article, we only consider the range $L < 1$. Also, we compute using $\beta = 10$ in all cases. There is every reason to expect that qualitatively similar findings will arise without these restrictions, at least for small enough Lewis numbers.

For large values of the parameter β the power law T^β in this model acts like the usual exponential law in combustion models, since $T^\beta = \exp(\beta \ln T) \sim \exp\big(\beta(T-1)\big)$ for T near unity, but it also has the numerically useful property of eliminating chemical reactivity at $T = 0$. We therefore avoid any need to introduce a 'cut off' temperature while still retaining the high thermal sensitivity of reaction rate that is essential for the phenomena we observe. An exponential Arrhenius law with a high activation energy would give qualitatively the same results, for which the value of β is then entirely equivalent to a Zeldovich number in the chemical kinetics.

non-burning solution

Because the reaction rate vector in (3) is precisely zero when $T = 0$ there is an exact non-burning solution that can be found for all values of $\delta < \infty$ and $\beta > 0$:

$$\begin{pmatrix} Y_{\rm F} \\ Y_{\rm X} \\ T \end{pmatrix} = \begin{pmatrix} Y_{\rm Ff}(y) \\ Y_{\rm Xf}(y) \\ T_{\rm f}(y) \end{pmatrix} = \begin{pmatrix} \frac{1}{2}\,\mathrm{erfc}\Big(-\sqrt{L/2}\,y\Big) \\ \frac{1}{2}\,\mathrm{erfc}\Big(\sqrt{L/2}\,y\Big) \\ 0 \end{pmatrix}. \tag{5}$$

That is, a power law dependence of chemical reactivity on temperature results in there being no finite Damköhler number for ignition $\delta_{\rm i}$, as there would be if the solution (5) were to cease to exist at some value of δ. The solution is also stable to infinitesimal perturbations for all values of $\delta < \infty$ and $\beta > 1$, so that, with β reasonably large, no finite Damköhler number for ignition $\delta_{\rm i}$ arises through the appearance of a linear or nonlinear instability of the cold solution.

burning solution for $\beta \to \infty$

For large enough values of δ, the model (3) with boundary conditions (4) also predicts the outer asymptotic diffusion flame structure as $\beta \to \infty$

$$T = T_{\rm b}(y) \sim \frac{1}{\sqrt{L}}\,\mathrm{erfc}\left(\frac{|y|}{\sqrt{2}}\right), \quad \begin{pmatrix} Y_{\rm F} \\ Y_{\rm X} \end{pmatrix} = \begin{pmatrix} Y_{\rm Fb}(y) \\ Y_{\rm Xb}(y) \end{pmatrix} \sim \begin{cases} \begin{pmatrix} \mathrm{erf}\Big(\sqrt{L/2}\,|y|\Big) \\ 0 \end{pmatrix} & : \ y > 0 \\ \begin{pmatrix} 0 \\ \mathrm{erf}\Big(\sqrt{L/2}\,|y|\Big) \end{pmatrix} & : \ y < 0 \end{cases} \tag{6}$$

with an inner problem that has the asymptotic form $T_{\rm b} \sim \big(1-\beta^{-1}\phi(\eta)\big)/\sqrt{L}$, with $\eta = \beta y\sqrt{2/\pi}$, in which $\phi(\eta)$ satisfies

$$\phi'' = D(\phi - \eta^2)e^{-\phi}, \qquad \phi'(\pm\infty) = \pm 1, \qquad D = \delta\,\frac{\pi}{4}\,L^{(3-\beta)/2}. \tag{7}$$

It is readily seen [13] that this problem has solutions (in fact two) if D is sufficiently large, but none if D becomes too small. Thus, in the asymptotic limit as $\beta \to \infty$, burning diffusion flame solutions fail to be found for values of $D < D_q$, or $\delta < \delta_{\rm q} \sim D_q \frac{4}{\pi} L^{(\beta-3)/2}$, where this inner problem ceases to have solutions.

boundary conditions for a flame edge

For values of δ larger than $\delta_{\rm q}$ both burning and non-burning solutions are possible. The triple flame or flame edge model (3)–(4) is then completed by specifying the boundary conditions

$$\lim_{x\to-\infty} \begin{pmatrix} Y_{\rm F} \\ Y_{\rm X} \\ T \end{pmatrix} = \begin{pmatrix} Y_{\rm Ff} \\ Y_{\rm Xf} \\ T_{\rm f} \end{pmatrix}, \quad \lim_{x\to\infty} \begin{pmatrix} Y_{\rm F} \\ Y_{\rm X} \\ T \end{pmatrix} = \begin{pmatrix} Y_{\rm Fb} \\ Y_{\rm Xb} \\ T_{\rm b} \end{pmatrix}, \quad T(t,0,0) = \tfrac{1}{2} \tag{8}$$

which represent a transition from a cold to a burning state, provided of course that the burnt solution exists. The system of equations can be studied in either a time dependent form, or in a specifically steady state form by taking

$$\frac{\partial}{\partial t} \equiv 0. \tag{9}$$

The condition in (8) which defines the origin to be a point where $T = \frac{1}{2}$ serves, in effect, to define the propagation speed S in equations (3). Because the problem is translationally invariant in x one is free to make any suitable choice for the position where $x = 0$. In steady state calculations S is then an eigenvalue of the nonlinear problem, while in unsteady calculations $S(t)$ becomes the time dependent function

$$S = \big(T_{xx} + \mathcal{R}\big)\Big/ T_x \quad \text{evaluated at} \quad x = y = 0. \tag{10}$$

This definition fails if $T(t,x,0)$ happens never to pass through the value $\frac{1}{2}$ or if $T_x(t,0,0)$ becomes equal to zero. In principle, another choice for the value of T at the origin could then be made, but for the calculations presented here this was never necessary.

Where the burnt solution does not exist, namely for $\delta < \delta_{\rm q}$, the boundary condition in (8) as $x \to \infty$ becomes meaningless. A variety of alternatives can be postulated. One is that a non-trivial steady solution might form having the cold solution (5) at both far field boundaries. Such

a solution could be specified using either a Neumann boundary condition or the cold Dirichlet boundary condition

$$\lim_{x\to\infty} \frac{\partial}{\partial x}\begin{pmatrix} Y_{\mathrm{F}} \\ Y_{\mathrm{X}} \\ T \end{pmatrix} = \begin{pmatrix} 0 \\ 0 \\ 0 \end{pmatrix} \quad \text{or} \quad \lim_{x\to\infty} \begin{pmatrix} Y_{\mathrm{F}} \\ Y_{\mathrm{X}} \\ T \end{pmatrix} = \begin{pmatrix} Y_{\mathrm{Ff}} \\ Y_{\mathrm{Xf}} \\ T_{\mathrm{f}} \end{pmatrix} \tag{11}$$

of which the former Neumann, or zero flux condition is more general since it can also apply where a burning solution does exist at the far field boundary. In most cases, this was the boundary condition employed in the calculations.

3 Numerical calculations

The sets of equations (3), (4) and (8) were solved numerically in a region having $X_{\min} \le x \le X_{\max}$ and $-Y \le y \le Y$ by using a spatial discretisation with bilinear quadrilateral elements. The grid was uniform in the x direction but had some grading in the y direction towards $y = 0$ where more rapid changes in the solution occur, essentially because of large reaction rates where the temperature is high. The element sizes in the y direction formed a geometric progression with an element adjacent to the centre line being up to eight times smaller than an element on the boundary. Some grading in the x direction may also be useful for steady state or steadily propagating solutions but is not appropriate, unless adapting itself to the solution, for temporally varying results. This level of sophistication seemed unnecessary, with interesting solutions being computed adequately using a fine enough uniform grid in the x direction.

The spatial discretisation resulted in a system of ordinary differential equations that were solved using a simple Euler code, taking account of the special condition (10) for computing the speed $S(t)$. A steady state code based on Newton iteration was also used, when appropriate, to solve the stationary ($S = 0$) or steadily propagating ($S =$ constant) equations.

Although the Dirichlet boundary conditions in (8) were imposed at $X_{\max}$ for calculating flame edges where the burning solution exists, all other results computed here were obtained by using the Neumann condition that appears first in (11). Since the actual boundary conditions of the model in (4), (8) and (11) are all applied at infinity, the objective in any one calculation is to arrive at a solution that, at least over a significant part of the spatial domain, is independent of the chosen finite size of the numerical domain for large enough values of $X_{\min}$, $X_{\max}$ and Y. The values $X_{\min} = -10$ and $Y = 5$, with their appropriate Dirichlet conditions applied, proved to be more than adequate in all cases.

However, because in some cases the rear Neumann boundary condition applied at $x = X_{\max}$ alters the solution from the form that it would otherwise adopt at that point in an unbounded domain, extra care needed to be exercised in choosing $X_{\max}$. For positive values of S, the effect of the rear boundary condition is felt within a boundary layer around $x = X_{\max}$, the thickness of which increases as S decreases. After some experimentation, a value of $X_{\max} = 30$ was found to produce solutions that were practically independent of the choice of $X_{\max}$ for values of x less than about 20 (often more) over most of the ranges of Damköhler and Lewis numbers that we wished to consider. Only in some cases that will be discussed later, having a very small positive value of S, was it impossible to find a value of $X_{\max}$ that would give solutions that are independent of the choice of $X_{\max}$—in fact the solution does depend on $X_{\max}$ in these cases.

A computational region for which $-10 \le x \le 30$ and $-5 \le y \le 5$ was therefore used in all calculations. In any one computation over this domain, a 400×40 grid gave essentially grid independent solutions to at least two significant figures. Grids of 200×20 and 800×80 were also used, the finest resolution being used to generate the plots describing particular flame solutions

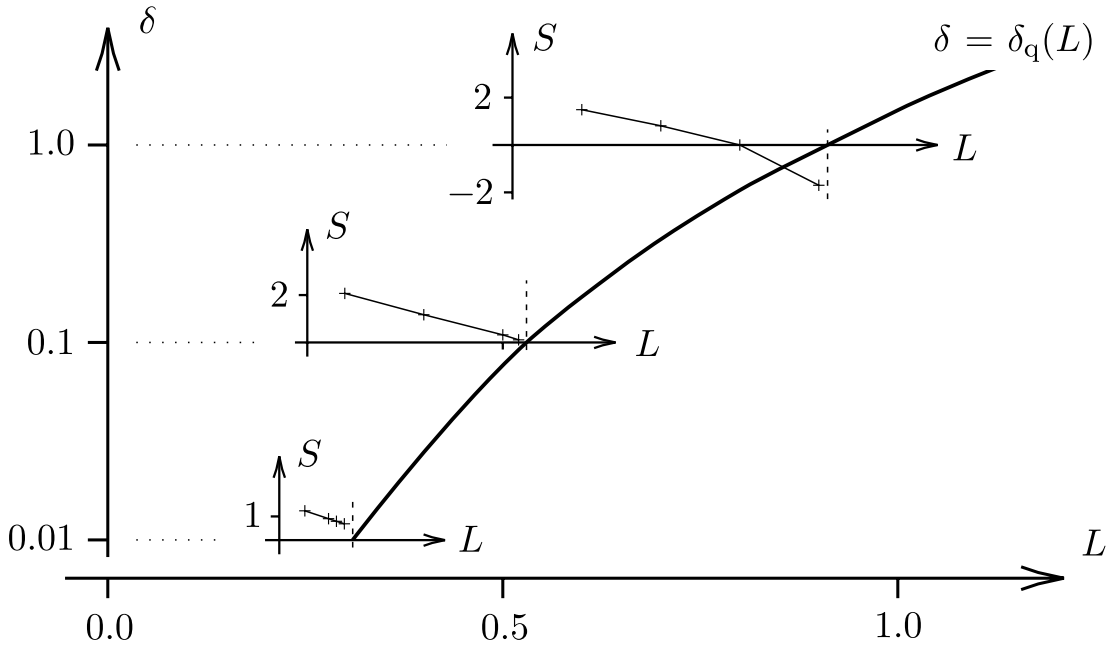

Figure 1: The quenching curve $\delta = \delta_{\rm q}(L)$, shown as the thick solid line, for $\beta = 10$. For each of the Damköhler numbers $\delta = 1.0$, $\delta = 0.1$ and $\delta = 0.01$ the sub-figures give the flame edge propagation speed S as functions of the Lewis number L. In the lowest sub-figure we find that $S\big(\delta_{\rm q}(L), L\big) \approx 0.57 > 0$.

shown in this article but taking as much as 4^4 times as long for a numerically stable calculation than the coarsest grid.

The cold and burning solutions $f_{\rm f}(y)$ and $f_{\rm b}(y)$, imposed where appropriate at $X_{\rm min}$ and $X_{\rm max}$, were obtained by setting $\mathcal{R}$ to 0 in (3) and solving the resultant two-point boundary value problem in the domain $-Y \le y \le Y$ using one dimensional linear finite elements on a mesh graded towards the centre line. Of course, when the Neumann condition was used at $X_{\rm max}$ only the cold solution was required and imposed at $X_{\rm min}$

4 Edge propagation where a diffusion flame exists

The numerically calculated path $\delta = \delta_{\rm q}(L)$ at which burning solutions cease to exist is shown as the thick solid curve in Figure 1. Time independent calculations of fully two dimensional flame edges can be carried out in the parameter space above this path, where $\delta > \delta_{\rm q}(L)$, revealing eigenvalue edge propagation speeds $S(\delta, L)$ for the solution in each case.

Of particular interest in these calculations is the behaviour of $S(\delta, L)$ as the quenching curve is approached. The sub-figures superimposed on figure 1 show how values of S change on three paths in (δ, L) space, each at fixed δ. A general trend is that values of S increase as the Damköhler number δ is increased and the Lewis number is reduced. This may be expected because the diffusion flame temperature $T_{\rm b}$ also increases. However, the effect of Lewis number is enhanced further by differential diffusion around the flame edge itself, producing even higher temperatures near the end of the diffusion flame. The effect is so dramatic that for low enough Lewis numbers, the propagation speed does not become negative even as the quenching curve $\delta = \delta_{\rm q}(L)$ is approached, as seen in the lowest sub-figure of figure 1.

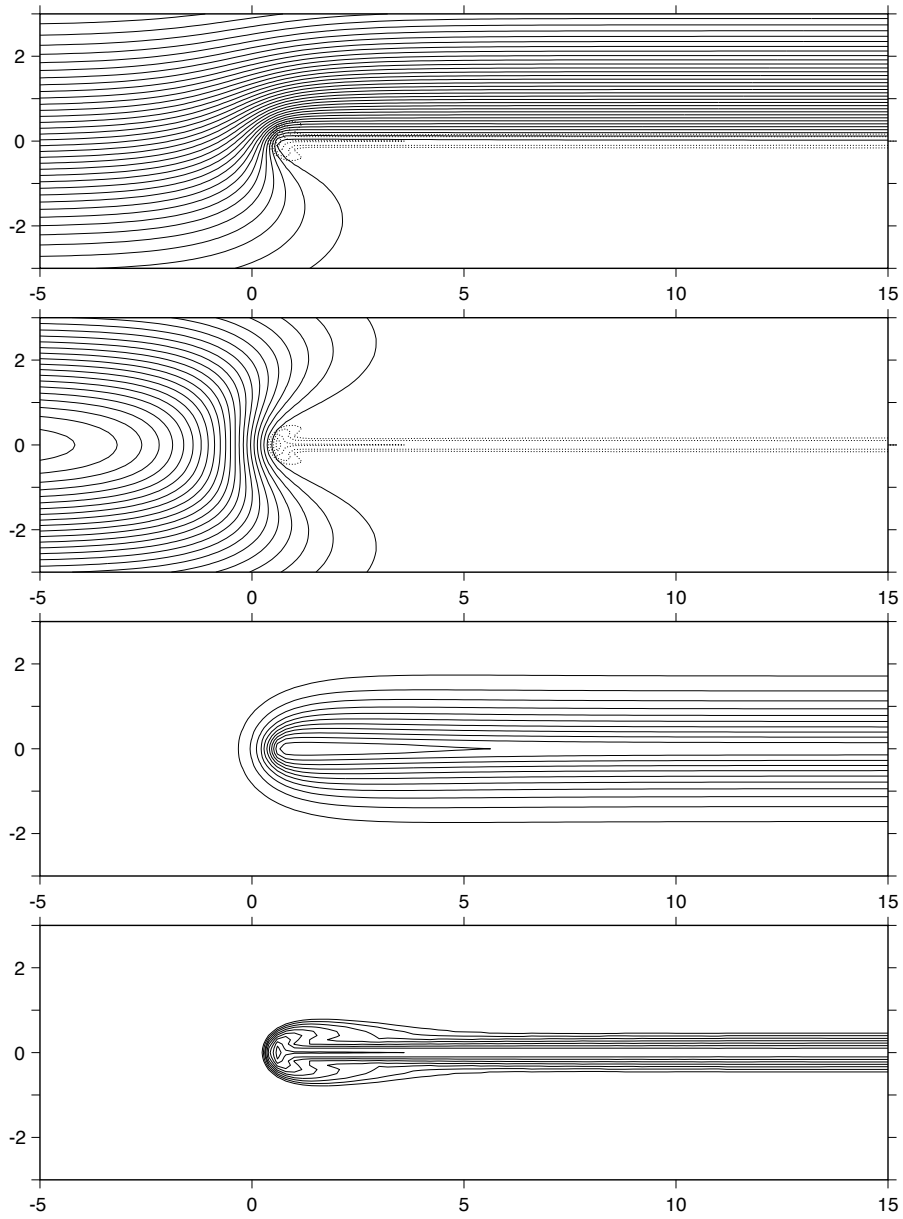

Figure 2: A flame edge calculated for $\delta = 0.01$ and $L = 0.2$, propagating steadily at a speed $S \approx 1.752$ and corresponding to the point marked A in figure 4. Shown from top to bottom are: contours of fuel concentration Y_{F} from 0 to 1 in steps of 0.025 (contours of Y_{X} would simply be reflected about $y = 0$); contours of the product $Y_{\mathrm{F}}Y_{\mathrm{X}}$ from 0 to 0.25 in steps of 0.01; contours of temperature T from 0 to its maximum value of 2.363 in steps of 0.2 (the maximum value of T for $x \geq 15$ is 2.124); and contours of the reaction rate $\delta\beta^3 Y_{\mathrm{F}}Y_{\mathrm{X}}T^{\beta}$, ordered in geometric progression from 2^{-4} and increasing by a factor of 2 from one contour to the next. Reaction rate contours above and including the value 2 are also shown as dotted lines in the upper two contour plots.

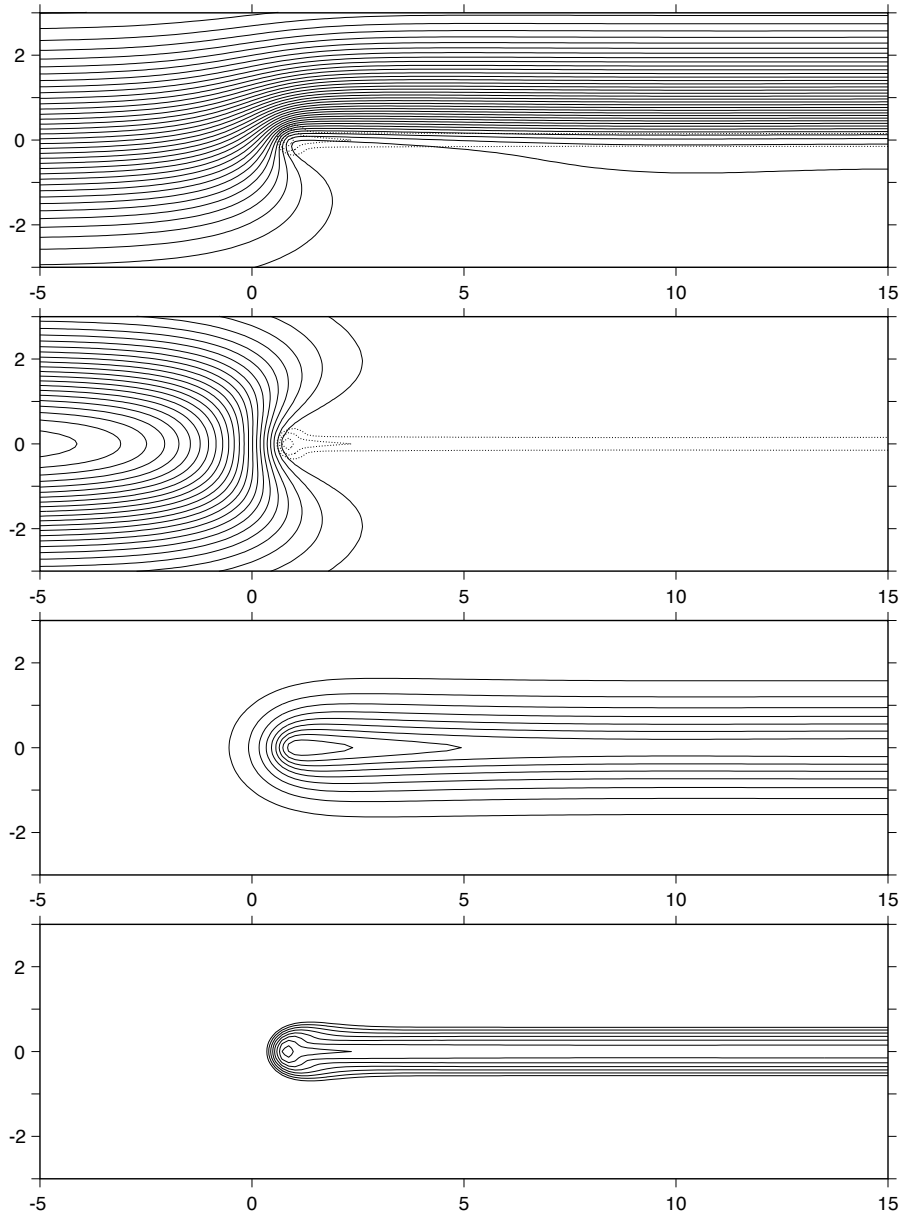

Figure 3: A flame edge calculated for $\delta = 0.01$ and $L = 0.3$, propagating steadily at a speed $S \approx 0.623$ and corresponding to the point marked B in figure 4. Shown from top to bottom are: contours of fuel concentration Y_{F} from 0 to 1 in steps of 0.025 (contours of Y_{X} would simply be reflected about $y = 0$); contours of the product $Y_{\mathrm{F}}Y_{\mathrm{X}}$ from 0 to 0.25 in steps of 0.01; contours of temperature T from 0 to its maximum value of 1.949 in steps of 0.2 (the maximum value of T for $x \geq 15$ is 1.513); and contours of the reaction rate $\delta\beta^3 Y_{\mathrm{F}}Y_{\mathrm{X}}T^{\beta}$, ordered in geometric progression from 2^{-4} and increasing by a factor of 2 from one contour to the next. Reaction rate contours above and including the value 2 are also shown as dotted lines in the upper two contour plots.

This is illustrated by the temperature contours shown in figures 2 and 3. The latter is calculated at a point that is almost on the quenching curve $\delta = \delta_q$ for a Damköhler number of $\delta = 0.01$, corresponding to the point marked B in figure 4, while the former has a lower Lewis number which sets it well away from the quenching curve, corresponding to the point marked A in figure 4.

In each of these figures, the top contour plots show how fuel leakage (and similarly oxidant leakage) occur ahead of the narrow region in which significant chemical reaction occurs, seen in the bottom contour plots or in the dotted reaction rate contours reproduced within the upper two contour plots. Well behind the flame edge, fuel and oxidant are inhibited from crossing the region of reaction, which is now a diffusion flame. However, the reaction rate in the diffusion flame is significantly weaker in figure 3 than it is in figure 2, so that some leakage of fuel and oxidant is noticeable in figure 3 away from the flame's leading edge. This is a feature of diffusion flames that becomes more noticeable as the point of quenching is approached [13]. The product $Y_F Y_X$ is a measure of the degree of mixing that has occurred between fuel and oxidant, and this is predominantly non-zero only ahead of the flame edge, as seen in the second plots of each figure. It can be seen that the solution in figure 2 which has a higher propagation speed involves a narrower region of premixing close to the leading edge of the region of significant chemical reaction.

Also, comparing the contours of fuel concentration and temperature, the spatial range over which temperature decreases is significantly smaller than the range over which the fuel concentration changes. This is a direct result of the greater diffusivity of reactant than temperature. A second effect of the enhanced diffusivity of reactant is that, in order to maintain a balance between the flux of reactants into the flame and the flux of heat out of it, the temperature must rise above the value it would have for Lewis numbers of unity. The effect is greater near the flame edge, where fluxes are two dimensional, than it is behind it, leading to a yet higher temperature in this region. The maximum diffusion flame temperature and the overall maximum flame temperature are respectively 2.124 and 2.363 in figure 2, and 1.513 and 1.949 in figure 3. The maximum diffusion flame temperatures are not far below their asymptotic limiting values given in equation (6) of $1/\sqrt{L}$, as $\beta \to \infty$, while, in each case, the flame edge has a noticeably higher maximum temperature than the temperature in the diffusion flame. The increase in maximum temperature above that in the diffusion flame is significantly greater near quenching, in figure 3, being 0.436 as opposed to 0.239 in figure 2.

This has a nonlinearly disproportionate effect on the reaction rate contours—the flame edge is able to maintain a strong degree of reactivity even though the diffusion flame itself in figure 3 is barely able to survive. As was seen in figure 1, for values of δ less than about 0.1, or L less than $L_C \approx 0.54$ (with $\beta = 10$), the enhanced reactivity of the flame edge is sufficient to sustain positive propagation as the quenching boundary $\delta = \delta_q$ is approached. Although the effect is not examined here, the critical Lewis number L_C below which positive edge propagation speeds are found on the quenching boundary should be expected to increase (while always remaining below unity) as the Zeldovich number β is increased.

5 Edge propagation where a diffusion flame cannot exist

This raises an interesting possibility: if a positive edge propagation speed arises at the quenching curve for $L < L_C$, can we suppose that the edge will continue to propagate even for $\delta < \delta_q(L)$ where the burning diffusion flame solution behind it can no longer exist?

One might speculate that such a flame edge could have cold boundary conditions at both $x = -\infty$ and at $x = \infty$, and it would then represent an edge that has entirely lost the flame to

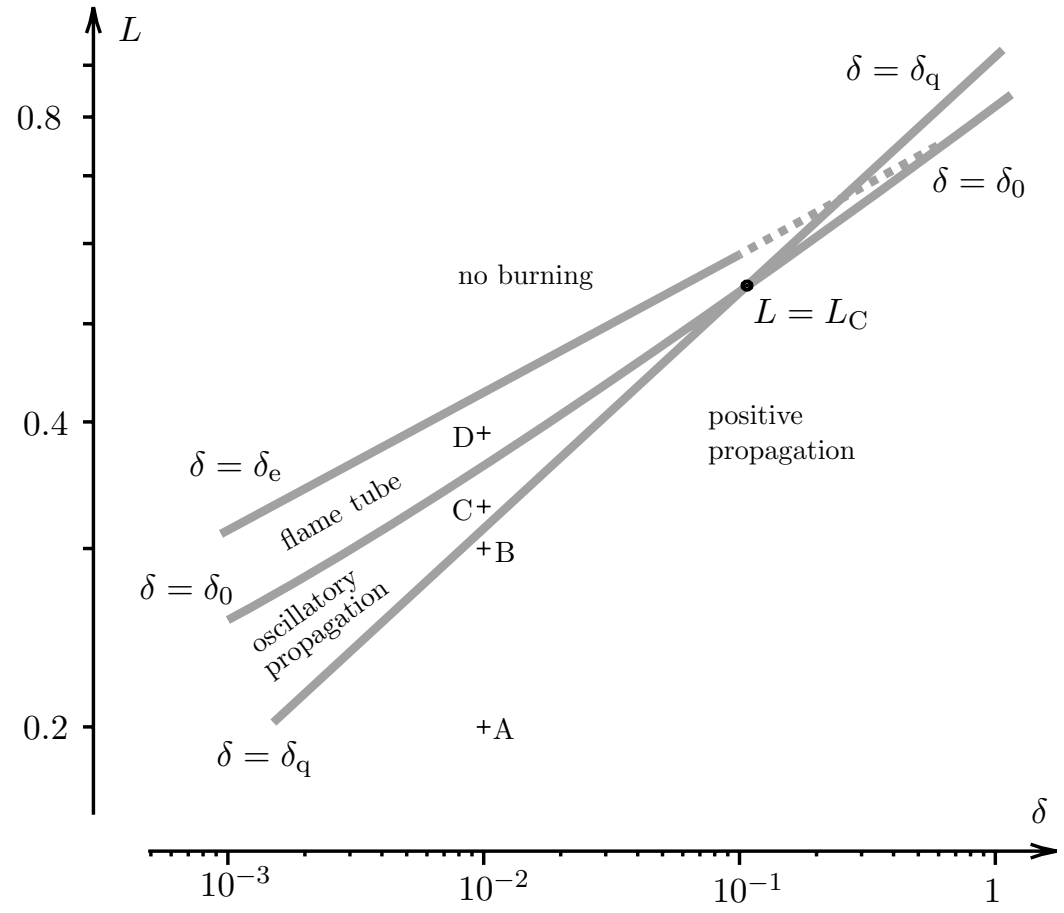

Figure 4: Boundaries in the space of Lewis number $L < 1$ and Damköhler number δ on which: *a)* a planar diffusion flame quenches $\delta = \delta_{\rm q}$; *b)* a flame edge has zero propagation speed $\delta = \delta_0$, the same curve continuing for $\delta < \delta_{\rm q}$ where it divides propagating edges from isolated stationary tubes of flame; *c)* flame tubes are extinguished $\delta = \delta_{\rm e}$ (the dotted part of this curve is still under investigation). The coarsest grid was used to obtain this mapping into different regions in parameter space, leading to an error of approximately the thickness of the grey lines when compared with solutions on the finer grids. The cross hairs marked A, B, C and D correspond to solutions described in other figures.

which it was attached. Our numerical investigation did not reveal the presence of any solutions of this nature for which $S \neq 0$, which does not mean that their existence can be ruled out entirely. It may be that we simply did not succeed in reaching an appropriate branch of solutions. It may also be that such solutions are unstable to time dependent perturbations which would have made them impossible to find using the time dependent approach which was normally used in calculations for which $\delta < \delta_{\rm q}$.

More specifically, an edge of a diffusion flame flame that cannot exist can no longer initiate a diffusion flame except perhaps as an unstable transient, or at least, as a time dependent, or a spatially varying form of non-premixed combustion. Kim [11] has shown that diffusion flames for small enough Lewis numbers with δ only slightly larger than $\delta_{\rm q}$ are unstable to disturbances that are periodic in x. Experiments by Ronney and co-workers [10] indicate that a fully developed form of such disturbances can continue to exist for $\delta < \delta_{\rm q}$. Such spatially varying forms of non-premixed combustion are clearly candidates for the end product of a flame edge that continues to advance with $\delta < \delta_{\rm q}$.

division of parameter space

Time dependent numerical investigations were carried out to examine the behaviour and effect of an advancing flame edge in the region of one dimensional flame quenching. Results show that the edge remains a robust part of the solution while the flame behind the edge ceases to exist as a steady uniform diffusion flame, at least for δ close enough to $\delta_{\rm q}$. Different forms of behaviour arise in the space of L and δ as mapped out in figure 4, the features of which will be discussed as we describe the different forms of solution that are found in each region. The boundaries identified in figure 4 were obtained by calculating many solutions at different values of δ and L using the coarsest grid. Differences of approximately the thickness of the lines drawn in the figure arise in the actual positions of the boundaries when checked against more finely resolved calculations. We are confident about the overall qualitative nature of the diagram except where the boundary $\delta = \delta_{\rm e}(L)$ is shown as a dotted line, as will be discussed at the end of this section.

As described already, diffusion flames exist for $\delta > \delta_{\rm q}(L)$. Edges of diffusion flames are found to propagate positively for $\delta > \delta_0(L)$ and negatively for $\delta < \delta_0(L)$, with the two bounding curves $\delta = \delta_{\rm q}(L)$ and $\delta = \delta_0(L)$ meeting at a point where $L = L_{\rm C}$. For any value of $L < L_{\rm C}$ the edge propagation speed $S(\delta, L)$ is positive as δ approaches $\delta_{\rm q}$ from above. The temperature and species profiles advance without change of form as shown in figures 2 and 3, which correspond to the points marked A and B in figure 4.

oscillatory flame edges

In reducing δ across the boundary $\delta = \delta_{\rm q}(L)$ the value of S, as defined in equation (10), becomes oscillatory. This is illustrated in figure 5. The oscillation is associated with a repeated breakup of the diffusion flame behind the first flame edge as illustrated in figures 6 to 10. As the leading edge continues to propagate it thus leaves successive regions of burning and non-burning that remain in its wake. These settle into a periodic pattern of flame tubes which do not propagate relative to the fluid and which sustain burning because of the elevated temperatures and enhanced reaction rates now found towards either side of each flame tube. A maximum in the propagation speed S is produced as the leading flame tube splits.

The successive plots in figures 6 to 10 are offset to highlight the way in which the edge moves to the left, at the speed shown in figure 5, leaving behind it a stationary pattern of flame tubes. In each case the data between $x = -10$ and $x = 25$ are relatively uninfluenced, to graphical

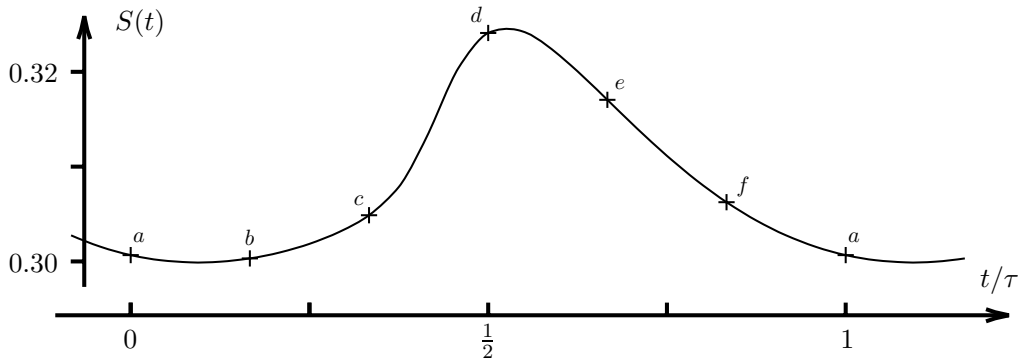

Figure 5: Oscillation of the edge propagation speed $S(t)$, over one period τ, for the case having $\delta = 0.01$ and $L = 0.33$ corresponding to the point marked C in figure 4. The fuel concentration $Y_{\rm F}$, degree of premixedness $Y_{\rm F}Y_{\rm X}$, temperature and reaction rate fields found at the times marked a, b, c, d, e and f are shown in figures 6 to 10.

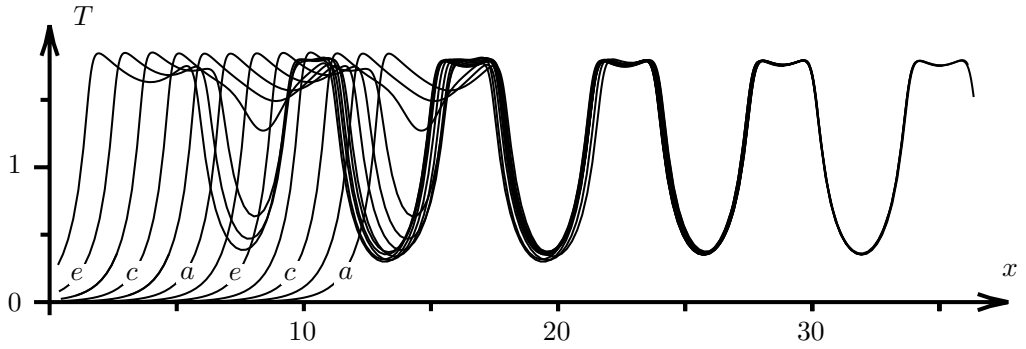

Figure 6: Temperatures measured along the centre line $y = 0$ at the times marked a, b, c, d, e and f in figure 5.

accuracy, by the Neumann boundary condition applied at $x = 30$. The effect of the boundary layer towards the right boundary where the choice of boundary condition has an influence, is found to be practically negligible in these calculations for $x \leq 25$. Only data in this range were used in plotting figures 6 to 10.

As in figures 2 and 3 the greater diffusivity of reactant than heat enhances the flame temperature near the propagating flame edge. It also enhances the temperature towards each side of each flame tube, allowing such structures to survive. The pattern in figures 6 to 10 involves features of both diffusion flames, which prevent fuel and oxidant from mixing, and combustionless mixing, as illustrated by the contours of $Y_{\rm F}Y_{\rm X}$ in figure 9. Within each tube, the chemical reaction, shown by the dotted contours of reaction rate, acts as a sink of fuel or oxidant. Outside the tubes, where the reaction is negligible, mixing can again take place. It is in these regions that the greater diffusivity of reactant than heat is responsible for the elevation of flame temperature, particularly towards the edges of each tube, which sustains the entire process.

As an unbounded periodic structure, this burning in flame tubes would appear to be a stable continuation of non-premixed burning below the quenching value $\delta = \delta_{\rm q}(L)$. It is likely that steady burning of this form would be possible over a wide range of stable wavelengths. Of course, the wavelength actually obtained via these computations is clearly determined by the dynamics of the propagation of the leading flame edge, and is therefore not arbitrary.

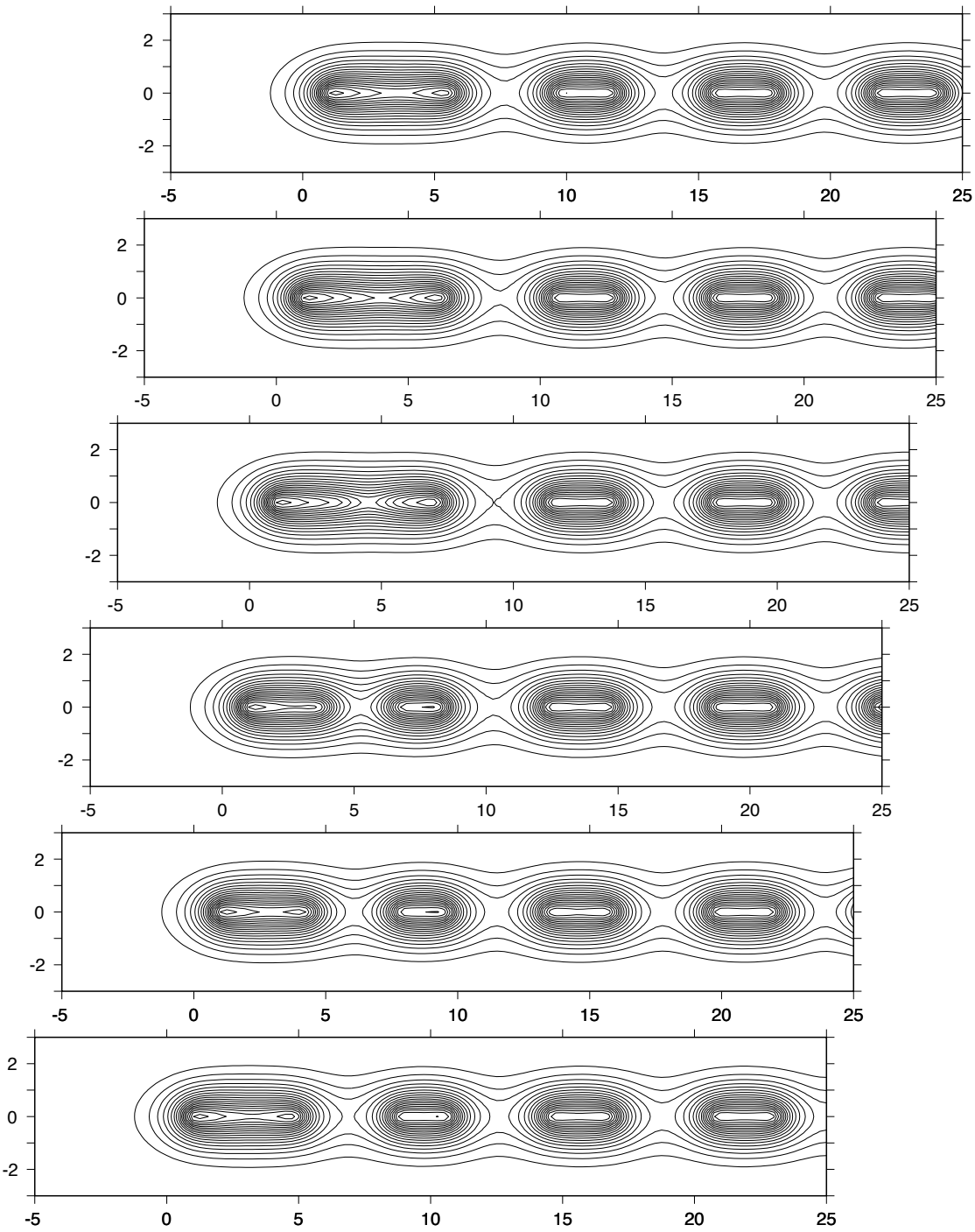

Figure 7: Time dependent behaviour of the temperature field following the flame edge in the case for which $\delta = 0.01$ and $L = 0.33$, corresponding to the point marked C in figure 4. Successive contour plots of temperature T, in steps of 0.1 starting from 0, are shown from top to bottom at the times marked a, b, c, d, e and f in figure 5.

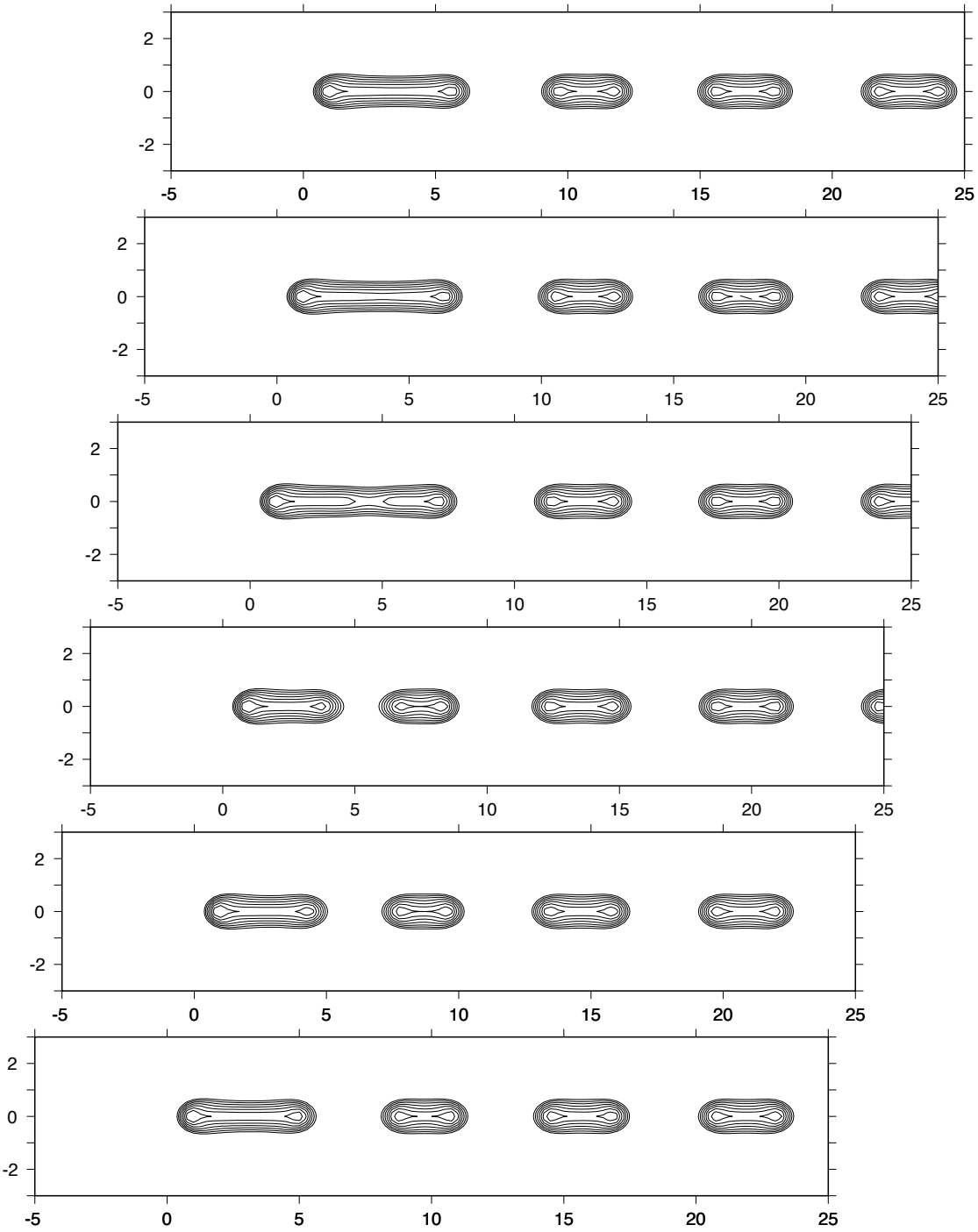

Figure 8: Time dependent behaviour of the reaction rate field following the flame edge in the case for which $\delta = 0.01$ and $L = 0.33$, corresponding to the point marked C in figure 4. Successive contour plots of $\delta\beta^3 Y_{\mathrm{F}} Y_{\mathrm{X}} T^{\beta}$, ordered to increase by a factor of 2 from one to the next, starting from 2^{-4}, are shown from top to bottom at the times marked a, b, c, d, e and f in figure 5.

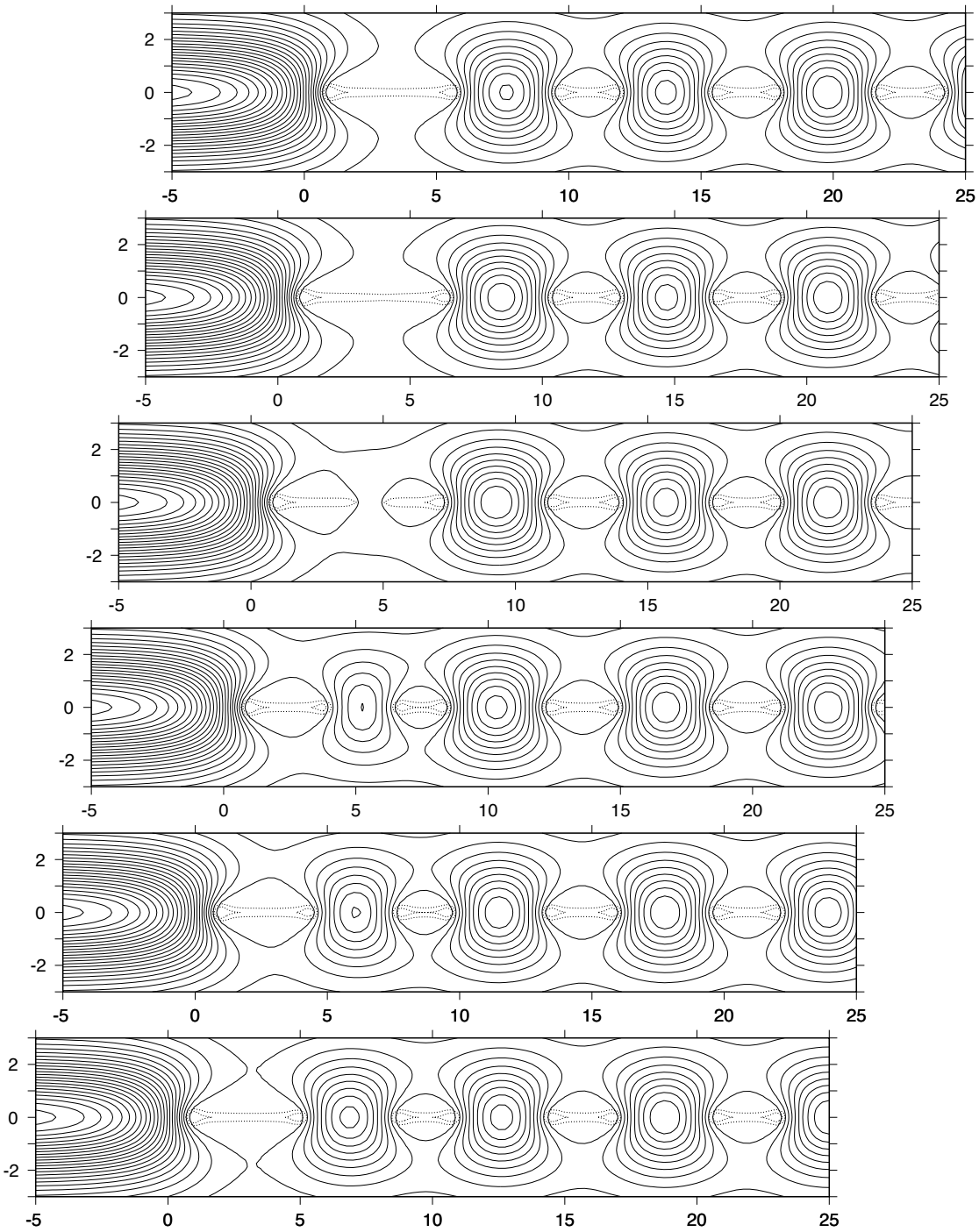

Figure 9: Time dependent behaviour of the premixedness field $Y_{\mathrm{F}}Y_{\mathrm{X}}$ following the flame edge in the case for which $\delta = 0.01$ and $L = 0.33$, corresponding to the point marked C in figure 4. Successive contour plots of the product $Y_{\mathrm{F}}Y_{\mathrm{X}}$, from 0 to 0.25 in steps of 0.01, are shown from top to bottom at the times marked a, b, c, d, e and f in figure 5. Reaction rate contours above and including the value 2 (as in figure 8) are also shown as dotted lines.

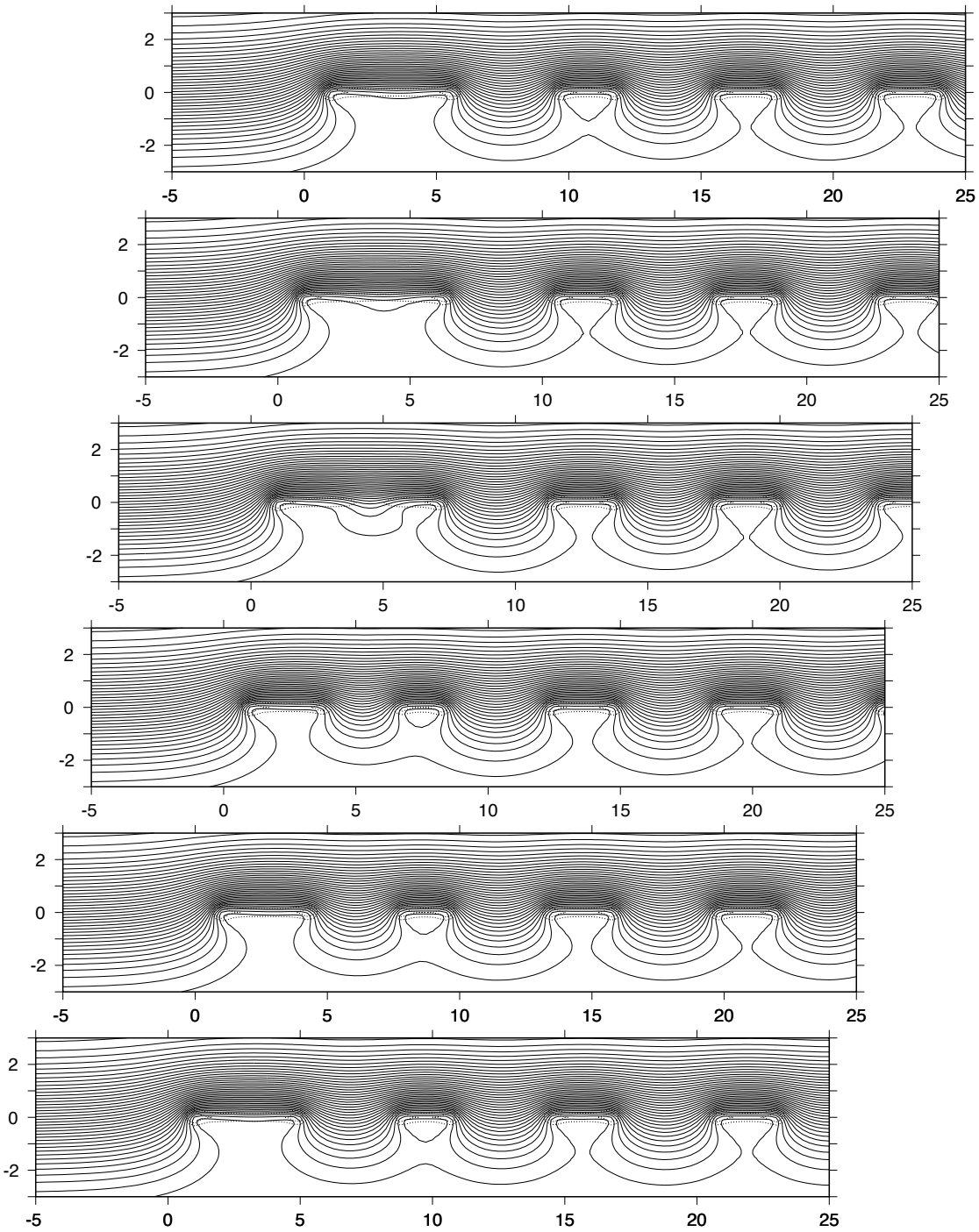

Figure 10: Time dependent behaviour of the fuel concentration field Y_F following the flame edge in the case for which $\delta = 0.01$ and $L = 0.33$, corresponding to the point marked C in figure 4. Successive contour plots of Y_F, from 0 to 1 in steps of 0.025, are shown from top to bottom at the times marked a, b, c, d, e and f in figure 5. Reaction rate contours above and including the value 2 (as in figure 8) are also shown as dotted lines.

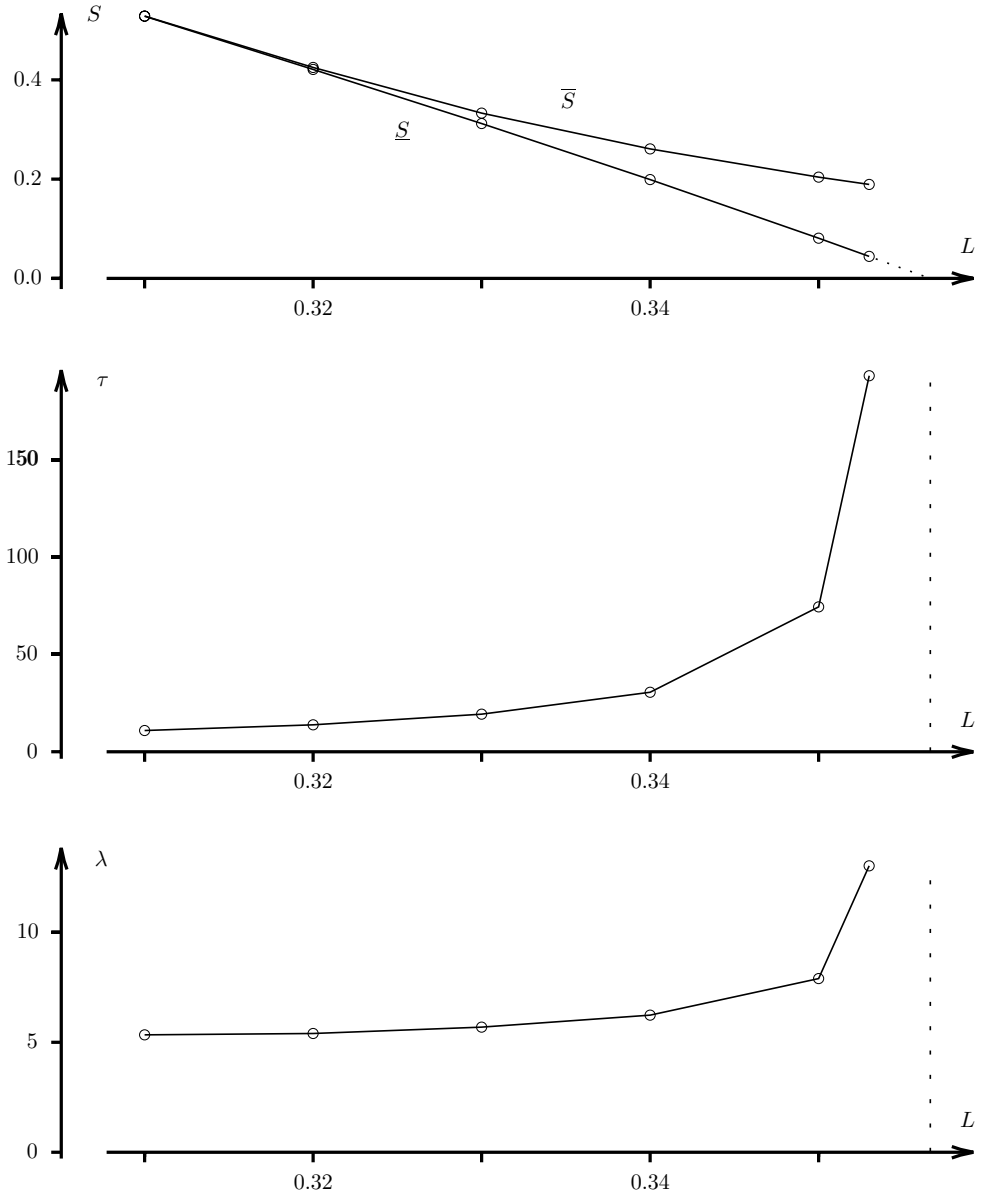

Figure 11: Variation with Lewis number L of the maximum propagation speed $\overline{S}$, the minimum propagation speed $\underline{S}$, the period of oscillation in the propagation speed τ and the wavelength λ of flame tubes that are created behind the flame edge. The Damköhler number is fixed at $\delta = 0.01$ in these calculations which were carried out using the intermediate grid.

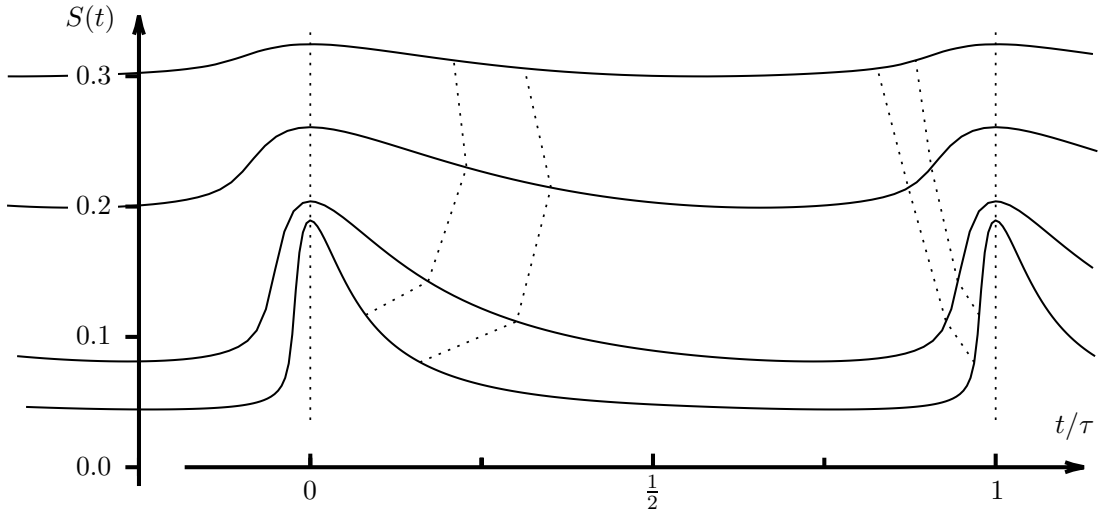

Figure 12: Oscillations of the edge propagation speed $S(t)$, over one period τ, for the cases having $\delta = 0.01$ and (from top to bottom) $L = 0.33$, $L = 0.34$, $L = 0.35$ and $L = 0.353$. Dotted lines trace the path of points where the flame speed is a maximum, has its median value, and has a value one quarter of the way from its minimum to its maximum.

In figure 11 we plot four quantities relating to the oscillatory edge propagation found over a range of Lewis numbers with a fixed value of $\delta = 0.01$. These are the maximum and minimum propagation speeds of the flame edge, the period in its oscillation and the wavelength of the flame tubes that are laid down by the flame edge as it moves on. It can be seen that the maximum and minimum propagation speeds start out almost identical towards the quenching boundary $\delta = \delta_{\rm q}$ and that they both decrease, becoming more and more disparate in value as the zero propagation speed boundary $\delta = \delta_0$ is approached. As this happens, the period of oscillation in the flame speed grows, apparently without limit, while the wavelength of the flame tubes laid down by the oscillating flame edge increases more gradually, but at an increasing rate.

non-propagating flame tubes

As L is increased towards a further boundary, the minimum edge propagation speed falls off towards zero and the period of oscillation grows towards infinity, as seen in figure 11. Towards this limit, figure 12 shows that the propagation speed tends to spend most of the oscillation close to its minimum value. Since S is also nearly zero at this stage, there is very little change that takes place over a long period of time, while the time spent near a maximum in the propagation speed, when the leading flame tube splits as seen in figures 5 to 10, becomes a decreasingly short portion of the overall oscillation. This indicates that the limit as the minimum propagation speed falls off to zero should involve a nonuniform convergence to an unchanging stationary solution, arising only from the solution at minimum propagation speed. Extrapolating from the results shown in figure 11 this should happen at a Lewis number of about $L \approx 0.357$ when the Damköhler number has the value $\delta = 0.01$. After this boundary, there should be no further propagation of flame tubes in a space that is unbounded in x and y. We will, for the moment, denote this boundary by $\delta = \delta_0'(L)$.

However, investigation of flame edge behaviour in appropriate ranges of parameters reveals that the boundary seems to be a continuation of the curve $\delta = \delta_0(L)$ corresponding to an edge propagation speed of zero for $\delta > \delta_{\rm q}$: for lower Damköhler numbers, $\delta < \delta_{\rm q}$, we still find $S = 0$

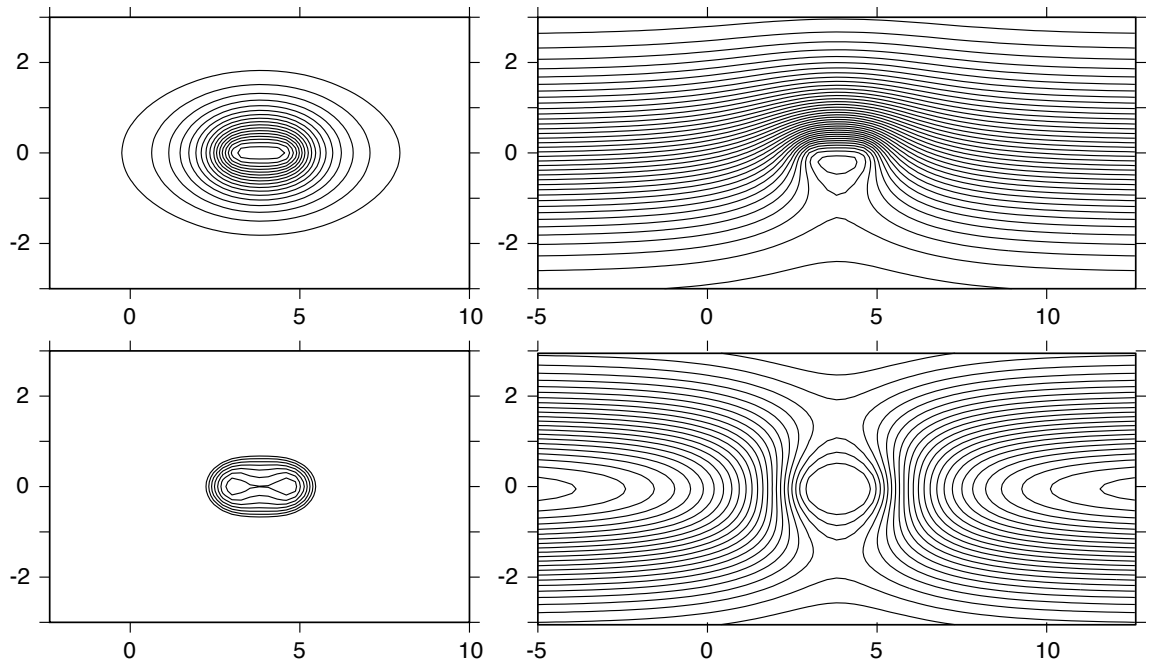

Figure 13: An isolated, stationary flame tube in the range $\delta_0 > \delta > \delta_e$ showing: temperature contours (upper left, in steps of 0.1 starting from 0); reaction rate contours (lower left, increasing by a factor of 2 starting from 2^{-4}); fuel concentration contours (upper right, from 0 to 1 in steps of 0.025); and contours of premixedness $Y_F Y_X$ (lower right, from 0 to 0.25 in steps of 0.01). The solution is calculated for $\delta = 0.01$ and $L = 0.39$, corresponding to the point marked D in figure 4.

on the path $\delta = \delta_0'$ which does not seem to be disjoint from the path $\delta = \delta_0$, within the accuracy obtained in the numerical calculations. There is certainly a consistency in the definitions of both paths so that a continuity between them across the quenching boundary does not appear out of place. Thus, although further investigations may be needed to establish this more firmly in the vicinity of the critical Lewis number L_C we will retain the same symbol δ_0, rather than δ_0', for $\delta < \delta_q$.

The temperature field does however change character in crossing into the range $\delta < \delta_0(L)$. As well as there being no edge propagation, it also seems that there are no longer any non-periodic stationary solutions containing multiple flame tubes within an unbounded space, as modelled by the equations and relevant boundary conditions (3) to (11). This statement is equivalent to asserting that the wavelength λ also becomes infinite as the boundary $\delta = \delta_0$ is approached. This is consistent with the trends seen in figure 11. In order to understand this point it is necessary to appreciate some of the differences that must arise between a finite domain in x, as is necessarily involved in the numerical calculations, and the unbounded physical domain that is implied by the model.

In continuing time dependent numerical calculations, after reducing δ or increasing L past the boundary $\delta = \delta_0(L)$, the values of $S(t)$ defined by equation (10) are found to approach a constant value as time progresses. Different forms of behaviour result from beginning a calculation in this range with only one flame tube present or with several. With only a single tube initially present, others being removed artificially if necessary, values of $S(t)$ are found to evolve towards the value zero reasonably quickly providing a numerically stationary solution involving only a single flame tube, as illustrated in figure 13. The solution remains practically unchanged by moving either

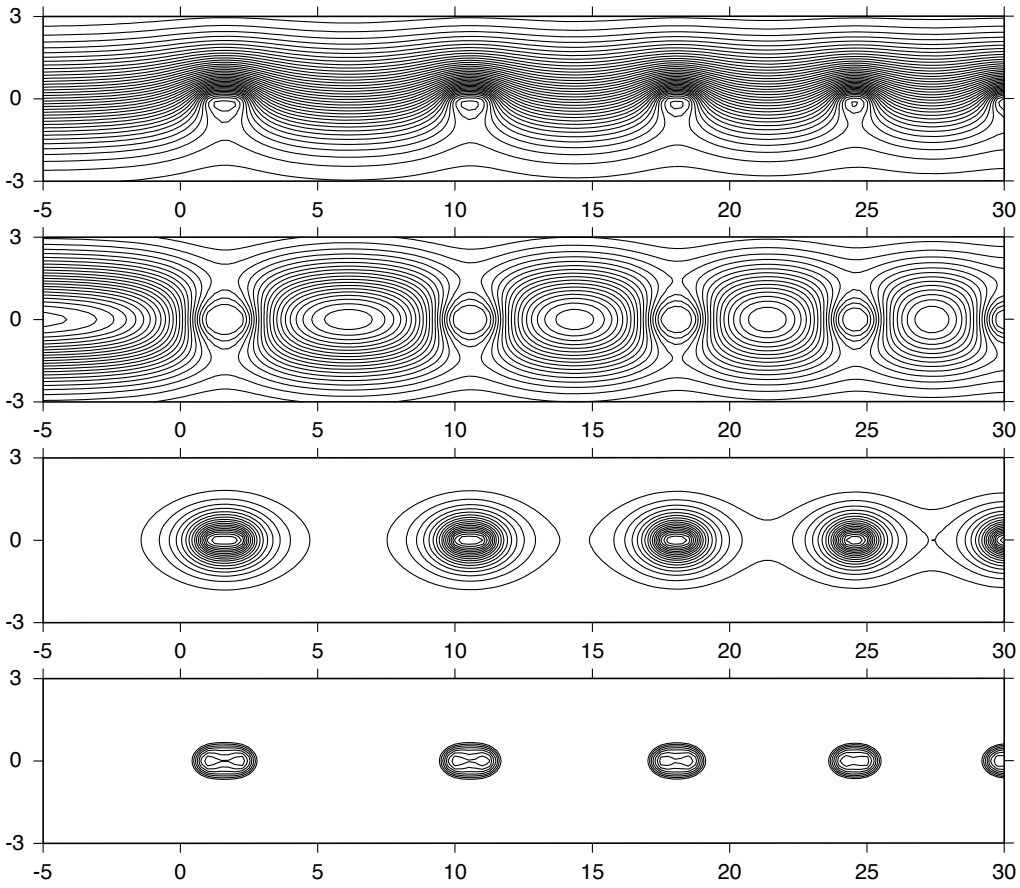

Figure 14: A sequence of flame tubes in the range $\delta_0 > \delta > \delta_e$, steadily propagating at the speed $S \approx 0.0098$, showing from the top: fuel concentration contours (from 0 to 1 in steps of 0.025); contours of premixedness $Y_F Y_X$ (from 0 to 0.25 in steps of 0.01); temperature contours (upper left, in steps of 0.1 starting from 0); and reaction rate contours (lower left, increasing by a factor of 2 starting from 2^{-4}). The solution is calculated for $\delta = 0.01$ and $L = 0.39$, corresponding to the point marked D in figure 4, and satisfies Neumann, or zero flux conditions at $x = 30$.

of the boundaries at $x = X_{\min}$ or $x = X_{\max}$ so that it does represent a genuinely isolated and non-propagating flame tube in an unbounded space. This solution has characteristics that are reminiscent of flame balls [12] in that it is non-propagating, isolated and sustained by reduced Lewis numbers.

Figure 14 illustrates the form of numerical solution that eventually arises when there are multiple tubes initially present in a calculation on a finite domain. As described earlier, this solution satisfies cold Dirichlet boundary conditions at $x = -10$ and Neumann conditions at $x = 30$. Exactly the same values of δ and L are used as in figure 13, corresponding to the same point marked D in figure 4. The calculation was started from an oscillatory evolution at a lower value of L. After a long time, the solution settles to a constant propagation speed S that is numerically non-zero ($S \approx 0.0098$). There are five flame tubes present in the calculation with the rightmost tube satisfying Neumann conditions at its right boundary.

Indeed, it seems that the Neumann, or zero flux condition helps to anchor the final flame tube to the right boundary. This prevents the tube from being advected out of the domain, and the non-zero propagation speed is then associated with the fact that the leading flame tube is

weakly asymmetric, as seen for example in the premixedness contours of figure 14. It is clear that the solution is not particularly relevant in an unbounded space. It depends intimately on the size of domain used in the calculation. Experimentally, of course, domains are finite with boundaries that could prevent flame tubes from migrating so that one might expect to find multiple stationary flame tubes in practise where conditions permit [10]. If the cold Dirichlet boundary condition in (11), rather than the Neumann condition, had been applied at the right boundary $x = X_{\max}$, then the rightmost flame tube would not have been anchored and we believe that a singe stationary flame tube would be the eventual outcome, although the solution could take a long time to calculate.

Different initial and boundary conditions from those involved in equations (8) to (11) certainly should be expected to lead to multiple flame tubes. For instance, periodic boundary conditions or Neumann conditions at both boundaries on a finite domain, would imply the presence of multiple peaks if any are found at all. A single flame tube is not therefore the only form of stationary burning solution that could arise naturally for $\delta < \delta_0$ and $\delta < \delta_q$. It is primarily a product of the choice of model and boundary conditions, as in (3) to (8) or (11). In general one would expect that individual tubes interact and move towards positions of equilibrium if suitable boundary conditions permit.

extinction

In continuing to reduce δ or to increase L, a further boundary $\delta = \delta_e$ is reached at which an isolated flame tube is extinguished. No burning at all is observed for $\delta < \delta_e$ and $\delta < \delta_q$.

The path of this boundary in figure 4 is still the subject of further investigation, in conjunction with a broader study of periodic and isolated flame tubes. The extinction boundary $\delta = \delta_e(L)$ does not converge on the quenching boundary $\delta = \delta_q(L)$ at the same point as $\delta = \delta_0(L)$. Indeed it does so for a larger value of δ and moreover it continues past the quenching boundary, as indicated by the dotted line in figure 4. Although the actual path of the boundary in this range is not yet known the form of the dotted line should at least be qualitatively correct. As a consequence, there is a range of Lewis numbers above L_C contained between the three boundaries $\delta = \delta_q$, $\delta = \delta_0$ and $\delta = \delta_e$. In this region, an isolated stationary flame tube can exist even though a uniform diffusion flame can also exist having an edge propagation speed that is negative. Daou and Liñán [8] have found such a range of isolated solutions in a study of premixed flame edges. We have also found solutions in the non-premixed case that are analogous to those illustrated in figure 13.

hysteresis

Once the flame is completely extinguished, increasing δ once again above δ_e will of course not bring it back to life. This is entirely precluded by the reaction rate law in this model for which the reaction rate is exactly zero for the quenched solution, so that it remains zero.

On the other hand, when increasing δ above δ_0 for $L < L_C$ with an isolated flame tube already in existence, one might expect some hysteresis. In fact we have not as yet observed this even with relatively fine increments in δ or L. The isolated flame tube loses stability to a flame edge with oscillatory propagation speed, as already described. Dynamically, this begins with a single splitting of the flame tube to produce two tubes that move apart each with a speed of $S(t) > 0$ relative to the medium, but in opposite directions. Following only the leftward propagating tube, as is implicit in the choice of origin in the conditions (8), a pattern of behaviour analogous to that shown in figures 5 to 10 is eventually produced. This lack of hysteresis is consistent with

there being a non-uniform convergence to an isolated flame tube when reducing δ towards $\delta = \delta_0$.

6 Conclusions

Using the example of a diffusion flame edge, or triple flame model, we have revealed that regimes of parameter space can arise in which:

- a burning solution ceases to exist in the form of a one dimensional structure as a boundary in parameter space is crossed
- nevertheless, at least as a part of the boundary is approached for low enough Lewis numbers, the flame edge has a propagation speed that advances the burning solution into regions that are not burning
- in crossing this boundary, the advancing flame edge remains a robust part of the solution
- the major change observed in crossing the boundary is the breakup of the flame behind the edge into periodic tubes of burning and non-burning
- this is accompanied by the appearance of an oscillatory element in the speed of propagation of the edge, with a succession of tubes of uniform width and separation being laid down behind the edge
- in crossing a second boundary the propagation speed of the flame edge disappears altogether; the only unbounded non-periodic stationary solution then consists of an isolated flame tube that arises as a nonuniform limit from the oscillatory solutions; there seems to be no hysteresis between the different solutions across this boundary
- isolated flame tubes also arise in a part of parameter space where a uniform diffusion flame can exist and where its edge has a negative speed of propagation.
- in continuing forwards across a third, final boundary the flame tube is extinguished leaving no combustion whatever.

Solutions of this nature were first reported in [7]. They were also subsequently reported for premixed counterflow combustion [8, 9] and have been observed experimentally [10].

In summary, flame edges that advance burning into non-burning still continue to exist when the flame behind them ceases to exist as a uniform structure. The burning that is produced has been found to take on a non-uniform character, at least in the examples studied here. The breakup of a diffusion flame into separated tubes of burning, below the point of quenching at low enough Lewis numbers, has been observed experimentally [10].

On a more speculative note, if there are any flame edges that propagate leaving only a cold solution in their wake for Lewis numbers below unity, these may possibly be found as a bifurcation from an isolated tube of burning. Alternatively, such flame edges might only be possible in the absence of the linear instability that leads to the formation of flame tubes. Another open question involves the nature of the connection with this linear instability of a uniform diffusion flame [9, 11] to periodic disturbances along the flame for $\delta > \delta_{\rm q}$. When there is such an instability, it can be anticipated that a bifurcation gives rise to solutions involving periodic tubes of burning with a range of possible wavelengths when $\delta < \delta_{\rm q}$. Periodic flame tube solutions might also exist at higher values of δ, perhaps even where there is no linear instability of a uniform diffusion flame, contributing to a possible hysteresis in the appearance of oscillatory

flame edge propagation. It seems plausible that there is some connection between positive edge propagation and the existence of periodic flame tubes.

Acknowledgements: The authors are grateful to Joel Daou for helpful comments and suggestions, to the EPSRC for financial support and to the IMA in Minneapolis for academic and computing support as well as hospitality.

References

[1] Dold, J. W., Hartley, L. J., Green, D. (1991) "Dynamics of laminar triple-flamelet structures in non-premixed turbulent combustion" in Dynamical Issues in Combustion Theory. Eds. P. C. Fife, A. A. Liñán and F. A. Williams. IMA Volumes in Mathematics and its Applications **35**, Springer Verlag. 83–105.

[2] J. W. Dold (1992) Ends of laminar flamelets, their structure, behaviour and implications. ERCOFTAC Summer School on Laminar and Turbulent Combustion. RWTH Aachen 1992. Also available as proceedings of NATO ASI, Cargese, Corsica 1999, PDE's in Models of Superfluidity, Superconductivity and Reacting Flows. Ed. H. Berestycki. Kluwer (to be published, 2000).

[3] Dold, J. W. (1994) Triple flames and flaming vortices. Invited review, ERCOFTAC Bulletin **20**. 38-41.

[4] Dold, J. W. (1997) Triple flames as agents for restructuring of diffusion flames. Prog. Astronautics and Aeronautics **173**. 61–72.

[5] Ju, Y., Matsumi, H., Takita, K., Masuya, G. (1999) Combined effects of radiation, flame curvature, and stretch on the extinction and bifurcations of cylindrical CH_4/air premixed flame. Combustion and Flame **116**. 580–592.

[6] Kioni, P. N., Rogg, B., Bray, K. N. C., Liñán, A. (1993) Flame spread in laminar mixing layers; the triple flame. Combustion and Flame **95**. 276–290.

[7] Thatcher, R. W., Dold, J. W., Cooper, M. (1998) Edges of flames that don't exist. 7^{th} International Conference on Numerical Combustion. York 1998. Book of abstracts. Mathematics Department, UMIST, U.K. p. 107.

[8] Daou, J., Liñán, A. (1998) The role of unequal diffusivities in ignition and extinction fronts in strained mixing layers, Combustion Theory and Modelling **2**. 449–477.

[9] Buckmaster, J. D., Short, M. (1999) Cellular instabilities, sublimit structures and edge-flames in premixed counterflows. Combustion Theory and Modelling **3**. 199–214.

[10] Kaiser, C., Liu, J-B. and Ronney, P. D. (2000) Diffusive-thermal instability of counterflow flames at low Lewis number, AIAA Paper No. 2000-0576, presented at the 38th AIAA Aerospace Sciences Meeting, Reno, NV, January 11–14, 2000.

[11] Kim, J. S. (1997) Linear analysis of diffusional-thermal instability in diffusion flames with Lewis numbers close to unity. Combustion Theory and Modelling **1**. 13–40.

[12] Zel'dovich, Ya. B., Barenblatt, G. I., Librovich, V. B., Makhviladze, G. M. (1985) The mathematical theory of combustion and explosions. Consultants Bureau, New York.

[13] Liñán, A.A. (1974) The asymptotic structure of counterflow diffusion flames for large activation energies. Acta Astronautica **1**. 1007–1039.